MET O 11 TECHNICAL NOTE NO 260

A LARGE AMPLITUDE GRAVITY WAVE IN THE LOWER STRATOSPHERE DETECTED BY RADIOSONDE

by

G.J. Shutts, M. Kitchen, P.H. Hoare*

* Meteorological Office, Shanwell, Tayside.

June 1987.

Met O 11 (Forecasting Research)
Meteorological Office,
London Road,
Bracknell,
Berkshire,
England.

E 54

A LARGE AMPLITUDE GRAVITY WAVE IN THE LOWER STRATOSPHERE DETECTED BY RADIOSONDE

by

G J Shutts, M Kitchen, P H Hoare*

Meteorological Office, Bracknell, Berkshire

* Meteorological Office, Shanwell, Tayside

June 1987

Abstract

Temperature profiles in the lower stratosphere commonly show fluctuations (typical peak-to peak amplitude of a few degrees) on a vertical scale of a few kilometres. The routine operational radiosonde launched from Shanwell (56.26N,2.52W) at 2318 GMT on 12th December 1986 recorded very large amplitude excursions in temperature (15.9 °K change over a vertical distance of 2 Km.) in the lower stratosphere which were identified as being exceptional by the staff at the radiosonde station.

The temperature fluctuations were accompanied by strong shear in the horizontal wind and large variations in the rate of ascent of the balloon. A rough estimate of the vertical momentum flux due to the gravity wave suggests a value of 3 or 4 Nm^{-2} over a horizontal scale of 20 Km. These observations, their meteorological context and interpretation are described in detail here.

1. Introduction

Detailed vertical profiles of wind and temperature measured by radiosondes have previously been used in studies of small scale structure in the atmosphere. For example, Corby (1957) used radiosonde observations to study gravity waves in the troposphere; Sawyer (1961) identified inertial oscillations of substantial amplitude in the lower stratosphere and Danielsen (1959) showed that the vertical structure of the atmosphere is laminated, with thin layers of high static stability sandwiched between almost isentropic layers. The humidity structure also shows such laminae. The United Kingdom (UK) RS3 radiosonde system provides highly reproducible temperature measurements combined with a very fast time constant of response (see Edge et al, 1986 and Nash and Schmidlin, 1987). Similarly, operational Cossor radar is capable of resolving fine structure in the horizontal wind profiles on a vertical scale of a few hundred metres and amplitude of $\simeq 1$ ms^{-1}. Much of the detail in the operational radiosonde sounding is discarded when the operational TEMP messages are composed but is clearly of value in research projects.

Whilst it is widely recognised that gravity wave breaking exerts a powerful influence on the middle atmospheric circulation, only recently has the influence of inertial-gravity wave motion on tropospheric flow been considered seriously by the numerical modellers. Unfortunately, the sort of information required by the modeller -large scale, area-averaged vertical momentum fluxes- are not available. Instead, most of our quantitative estimates of the intensity of gravity wave momentum transport derive from a few aircraft studies, often measuring extreme

fluxes over extreme orography(e.g. Lilly and Kennedy,1973).The case study presented here similarly deals with an extreme gravity wave event though over mountains of modest stature.Since this study demonstates the usefulness of routine soundings for quantifying gravity wave activity,it may,through regular analysis,be possible to build up a broader scale picture of the frequency , intensity and geographical distribution of gravity wave events.Such a viewpoint is clearly stated in Corby(1957),Reid(1972) and Lalas and Einaudi(1980):further relevant observational studies are described in the review paper of Nicholls(1973).Reid actually produced statistics on the frequency of occurrence of gravity waves at heights of 2 and 14 Kms. obtained from 500 ascents made at Shanwell.

Section 2 discusses the observational details and synoptic background to the gravity wave event which forms the principal theme of this paper.In Section 3,a simple model of finite amplitude gravity wave motion is used to interpret the balloon observations and various physical scenarios are considered to explain the character of the wave motion.The magnitude of the implied momentum flux is discussed in Section 4 with respect to current interest in gravity wave drag and some concluding remarks are made in Section 5 .

2. The Observations

a) The Shanwell Radiosonde Ascent

The detailed profiles of temperature and horizontal wind measured by the radiosonde launched from Shanwell at 2318 GMT on 12th December 1986

are shown in Fig. 1 and are derived from the RS3 radiosonde system fine structure archive . This dataset consists of turning points in the temperature and wind profiles and, as can be seen from Fig. 1, a considerable level of detail in the stratospheric profiles is obtainable.

Between 15.5 and 22 Km., the radiosonde encountered strong vertical gradients in the temperature and wind field. In particular,at the stable layer around 15.7 Km. altitude, the measured temperature increased by 9.9 ^{o}K for a change in the computed geopotential height of 134m. The minimum lapse rate recorded within this layer was - 0.3 $^{o}K.m^{-1}$; the two temperature measurements concerned were separated in time by about 5 seconds. At these altitudes, the time constant of response for the RS3 radiosonde temperature sensor is <1 second (see Nash and Schmidlin, 1987). This very stable layer was followed by an essentially isentropic layer of about 2 Km. deep (see inset profile of potential temperature, θ , in Fig 1(a).) and over this layer, the total fall in temperature was 15.9 degrees. Above 18 Km., another very stable layer was encountered, although not as sharp as that at 15.7 Km., followed by a deep layer with an average lapse rate of approximately 5 $^{o}K.Km^{-1}$ but interrupted by 3 small inversions. The radiosonde balloon burst at an altitude of 24.1 Km.

These large temperature variations were accompanied by strong vertical shear in the horizontal wind speed profile. The bases of the two very stable layers identified above were both associated with local maxima in the wind speed profile (see Fig. 1(b)) and the isentropic layer was a region of much lighter winds. The transition between the intense stable layer and the isentropic layer around 15.7 Km. altitude

was marked by a negative shear in the windspeed of about - 0.034 s^{-1} and a direction change of 22 degrees over the same layer(Fig.1(c)).

A plot of the radiosonde pressure measurements against elapsed time into flight revealed significant variations in the balloon ascent rate in the stratosphere. The rate of ascent computed from the change in radiosonde geopotential with time between adjacent data points in the fine structure archived data is plotted in Fig. 1(d). The mean rate of ascent of the balloon through the stratosphere was about 6 ms^{-1} but imposed upon this mean value were variations of ± 6ms^{-1}. In the two stable layers bounding the isentropic layer, the ascent rate was observed to fall to close to zero, whereas in the isentropic layer itself, the ascent rate was enhanced by over 5 ms^{-1}. That these variations were real is proved by examination of the data from the Cossor wind-finding radar. The rates of ascent from the radar data were computed as averages over (approximately) one minute intervals. A detailed specification of the Cossor radar angular and range measurements is quoted in Edge et al, 1986. The specification suggests that the reproducibility of the elevation angle measurements should be <0.1 degrees which would suggest an uncertainty in rate of ascent (averaged over one minute at a range of order 100 Km.) of <3 ms^{-1}. The radar should therefore be capable of resolving variations in ascent rate on the scale found here.

The close agreement between the rates of ascent computed from the two completely independent data sources confirms the presence of the variations described above.

Although there is no doubt that the ascent rate of the balloon was modulated in the stratosphere, a more difficult question is whether the

ascent rate variations can be used to infer the vertical velocity of the air encountered by the balloon. Lalas and Einaudi (1980) identified three potential sources of error in such inferred vertical velocities; these were:-

i) the ascent rate is directly dependent upon the air density

ii) abrupt changes in the drag coefficient of the balloon may occur in response to changes in the wind-shear experienced by the balloon

iii) changes in the drag caused by changes in the balloon radius because of changes in the air density, for example in inversion layers.

This latter effect is complicated by the gas within the balloon not being in thermal equilibrium with the atmosphere.

Lalas and Einaudi estimated the uncertainty in the vertical velocity deduced from the rate of ascent of a radiosonde balloons in the troposphere due to the effects i-iii above. They concluded that these effects could account for only a small part of the observed variations in the ascent rate. However, it should be noted that in their experiments, the magnitude of the ascent rate variations, the wind-shear and the temperature fluctuations were all much smaller than those recorded for the present data. Reid(1972) examined records from 500 radiosonde ascents from Shanwell looking for evidence of gravity wave activity in observed ascent rate variations. He considered the effect of changes in balloon drag coefficient on his results and was able to use

an independent measurement of the vertical velocity of the balloon relative to the air in order to quantify the errors. Reid was able to show that the ascent rate variations (typical amplitude $\simeq 1$ ms^{-1}) were primarily due to gravity waves. Thus, the literature provides no evidence to suggest that the large variations in ascent rate in the present data are not accurately reflecting substantial vertical velocities in the wind field.

b) The Meteorological Background to the Observations

The trajectory of the radiosonde ascent described above was calculated from the radar tracking data and its horizontal projection is plotted in Fig 2. At the time that the large amplitude disturbances were encountered in the stratosphere, the balloon was about 50 Km. from the eastern flank of the Cairngorm mountains. A feature of the horizontal wind profile measured during this ascent was the strong low level flow: at 1.9 Km. altitude, the windspeed was 35 ms^{-1} - a speed not exceeded thereafter until the balloon achieved an altitude of 7 Km. (Fig. 1(b)). The synoptic situation at the time of these observations is illustrated in Fig 3 which shows a sea-level pressure analysis over the United Kingdom at 0000 GMT on 12th December, 1986. An occlusion was orientated approximately north-south through Scotland and the surface position of the front at this time was analysed to be about 80 Km. west of Shanwell.

The features in the stratospheric temperature and wind profiles shown in Fig. 1 were ephemeral in nature: the radiosonde ascents launched at 1117 GMT on 12th December and 1118 GMT on the 13th December 1986 from Shanwell do not show evidence of abnormally large amplitude

wave activity (Fig 4). Maximum peak to peak amplitudes in temperature (on a vertical scale of a few kilometres) were about 6 °K compared to 16 °K for the intermediate(midnight) ascent. A time series of wind profiles recorded at Shanwell during this period(Fig.5) exhibit rather poor temporal correlation on vertical scales of less than a few kilometres. However, the ascents at 1715 and 2318 GMT on the 12th December both show considerable wind speed variability in the lower stratosphere. Looking further afield, the radiosonde launched from Long Kesh (54.48N,6.10W, Fig.6) at 2326 GMT on the 12th December recorded a layer between 14.8 and 16.7 Km. altitude where the temperature fell by 10.5 degrees at an average lapse rate of about 5 °K.Km^{-1} .In contrast to the Shanwell ascent, neither the wind speed nor the ascent rate show the same degree of variation on the scale of the temperature fluctuation though there are small local wind speed maxima in the stable layers at 14 and 18.7 Km.Similarly the radiosonde launched from Aughton(53.55 °N 2.92 °W,see Fig.3 for geographical location) at 0008 GMT on December 13 showed marked alternations of stable and nearly neutral layers yet no obviously coherent fluctuation in wind speed(Fig.7) and ascent rate(not shown).It appears therefore that the presence of large temperature fluctuations and nearly isentropic layers in the lower stratosphere does not necessarily indicate that the balloon has passed through a gravity wave;only when supported by ascent rate variations can the existence of gravity wave activity at the observation time be confirmed.

3. Theoretical interpretation

The observed temperature and wind fluctuation described in Section 2 is strongly suggestive of an internal gravity wave close to its 'saturation' amplitude -the point at which it may break through convective instability. Fig. 8 shows the distribution of streamlines computed for steady flow over a bell-shaped mountain at the onset of convective overturning taken from Lilly and Klemp(1979). The undisturbed flow is assumed to have uniform speed U and static stability B and compressibility effects are neglected. The streamlines may be thought of as isentropes and so the point marked by a cross has zero static stability. The main features of this large amplitude gravity wave solution are:

(1) deep layers characterised by weak stability, light horizontal winds and strong upward motion.

(2) shallower layers of intense stability, strong horizontal winds and downward motion.

(3) a pattern of ridges and troughs which tilt upstream with height.

Fig. 8 is a special case of a solution of Long's equation:

$$\frac{\delta^2\delta}{\delta x^2} + \frac{\delta^2\delta}{\delta z^2} + \frac{N^2}{U^2}\,\delta = 0 \qquad \text{----(1)}$$

where $\delta(x,z)$ is the vertical displacement of a streamline from its undisturbed height, (see Scorer, 1979). Eq. 1 is linear yet, under conditions of uniform wind speed, incompressibility and two-

dimensionality, its solutions are exact. A simple solution satisfying Eq. 1 is:

$$\delta(x,z)=a.\sin(kx+mz) \qquad \text{------(2)}$$

such that:

$$m^2=N^2/U^2-k^2 \qquad \text{-------(3)}$$

and represents an upward energy radiating wave with displacement amplitude 'a' and with horizontal and vertical wavenumber components k and m respectively. The horizontal and vertical components of the wind u and w respectively are given by:

$$u=U(1-\delta\delta/\delta z) \quad \text{and} \quad w=U\delta\delta/\delta x \qquad \text{----(4)}$$

implying that stagnation points , where u=0, will appear if $am \geq 1$ or, for hydrostatic waves ($m^2 >> k^2$) when:

$$aN/U \geq 1 \qquad \text{------ (5).}$$

Since the rate of mass flow between two stationary isentropic surfaces is fixed, the point at which u=0 corresponds to $d\theta/dz=0$ where θ is the potential temperature. If $\phi=\ln\theta$, then $d\phi/dz$ is the local stability and it may be shown that:

$$\phi=\phi_o+B(z-\delta) \qquad \text{-------(6)}$$

where ϕ_o is a constant reference value of ϕ. The onset of wave breaking occurs at the saturation amplitude a=N/U; the inequality in (5) corresponds to supersaturation. We will now use this sinusoidal wave solution to model the ascent of an idealised radiosonde balloon through a uniform airstream with gravity wave. It will be assumed that the balloon travels with the velocity of the ambient flow plus an upward component W equal to the rate of ascent of the balloon in an atmosphere at rest. Using Eqs. (2) and (4) the coordinates of the the balloon (x,z) satisfy:

$$dx/dt=U(1-a\cos(\chi t)) \qquad ----(7)$$

$$dz/dt=W+Ua\cos(\chi t) \qquad ----(8)$$

where $\chi t=kx+mz$ is the phase of the wave (see also Lalas and Einaudi, 1980). Multiplying (7) and (8) by k and m respectively and then adding the resulting equations gives:

$d(kx+mz)/dt=Uk+Wm$ so that :

$$\chi=Uk+Wm \qquad -----(9)$$

where the integration constant has been set to zero.

The ascent curve for $\phi(x,z)$ perceived by the balloon is then given parametrically by the two equations:

$$\phi=\phi_o+B(Wt+a(Uk/\chi-1)\sin\chi t) \qquad ----(10)$$

$$z=Wt+Uak\sin(\chi t)/\chi \qquad ----(11).$$

The stability measured by the balloon is obtained by dividing $d\phi/dt$ by dz/dt and can be shown to be given by:

$$d\phi/dz=B(1-am\cos\chi t)/(1+Uak\cos(\chi t)/W) \qquad ----(12)$$

from which it can be seen that the actual stability (the numerator of Eq.12) is modified by the factor $1/(1+w/W)$. The fact that the stability computed from an ascent could be significantly different from the actual stability was recognised by Scorer(1953) and was used ,by Corby(1957), to correct real soundings. Fig.9 shows the difference between the profile of potential temperature at x=0 and the profile seen by a balloon, for the following parameter values(which will be shown to fit the wave under consideration here):

$W=6$ m/s $U=20$ m/s $N=2.12.10^{-2}$ s^{-1}

$k=2\pi/20$Km

choosing'a' such that $Uak/W=1$ and using Eq.3 for m. The balloon perceives a markedly different 'vertical wavelength' as it samples phase variation in its horizontal as well as vertical motion. Where the downward motion of the air becomes comparable in speed with the balloon's ascent rate, a marked fictitious inversion appears. For instance, when $w=-W$ the balloon is no longer ascending yet it will still record changing θ values as it

moves horizontally through the stationary wave field. The marked inversion near 15.7 Km. in Fig. 1(a) is related to the decreased ascent rate of the balloon to close to zero; even so a highly stable layer is still implied. In addition to these shallow stable layers, there are nearly isentropic layers where the balloon travels upwards at almost twice its 'still air' ascent rate.

Denoting the rate of change following the balloon by D/Dt_B and that following an air parcel by D/Dt then:

$$D\phi/Dt_B = D\phi/Dt + W\delta\phi/\delta z \quad \text{so that}$$

$$D\phi/Dt_B = W\delta\phi/\delta z \quad \text{for adiabatic motion.}$$

Therefore the mean static stability averaged between times t_1 and t_2 is given by:

$$(\phi(t_2)-\phi(t_1)/W.(t_2-t_1)$$

assuming a constant ascent rate in still air. The real thickness of the stable layer near 15.7Km. is $W(t_2-t_1)$ which can be shown to be about 360m. and implies a static stability about three times smaller than the apparent stability in Fig. 1(a). Since the rate of ascent of the balloon in the layer of weak stability between 16 and 18 Km. rises to ≈11 m/s, the apparent stability is about one half of the actual stability there.

Determination of the vertical wavelength of the gravity wave and relating this to the dispersion equation (3) is complicated by the slantwise ascent of the balloon (typically 1 in 5). The apparent wavelength in Fig.1(a) will be a mix of horizontal and vertical phase variations as in Fig.9. From Eq.11 the apparent vertical wavelength equals $2\pi W/\chi$ so that the apparent vertical wavenumber m_* is given by:

$$m_* = Uk/W + m \qquad \text{-------- (13).}$$

Using Eq.(3) together with the substitution $k = N.\sin(\psi)/U$ leads to the following expression for ψ (the zenith angle of the wavenumber vector):

$$\psi = \sin^{-1}(m_* WU/N\Delta) - \epsilon \qquad \text{------(14)}$$

where $\Delta = (U^2+W^2)^{1/2}$ and $\epsilon = \tan^{-1}(W/U)$. We now go on to discuss some possible scenarios using the above formulae to provide quantitative estimates of vertical and horizontal wavelengths.

(a) <u>Stationary, hydrostatic, long wave (non-rotating)</u>

Consider k to sufficiently small in Eq.13 for $m_* = N/U$. Taking $N = 2.12.10^{-2}$ s^{-1} (consistent with the stability of an isothermal stratosphere with temperature equal to -60°C) and U=20 m/s gives a vertical wavelength $(2\pi/m_*) = 5.9$ Km. which does not agree with the apparent wavelength of the observed wave. Note that we have ignored possible Coriolis effects: these will be considered later.

(b) Stationary, non-hydrostatic or short, hydrostatic wave

(a) shows that if the gravity wave is assumed stationary, then k cannot be considered small -either because the wave is non-hydrostatic or because of horizontal phase variation along the path of the balloon. Using Eq. 14 , m and k may be calculated from ψ using the relations:

$$k=N.\sin(\psi)/U \quad \text{and} \quad m=N.\cos(\psi)/U \qquad ----(15)$$

given observed values of N, U, W and m_*. From Fig. 1(a) , we consider an apparent vertical wavelength to extend between 15.8 and 18.5 Km. and take $N=2.12.10^{-2}m^{-1}$ and W=6 m/s. The following values of U give the corresponding horizontal and vertical wavelengths(λ_x and λ_z respectively):

U(m/s)	λ_x(Km)	λ_z(Km)
18	15.39	5.69
20	15.59	6.41
25	16.67	8.27
30	18.35	10.16

Since the $\lambda_x^2 >> \lambda_z^2$ for wind speeds less than 25 ms^{-1}, the corresponding waves are hydrostatic to a reasonable degree of approximation. An independent check on the ratio of the horizontal to

vertical wavelengths is provided by the ratio of the amplitudes of w and u' (=u-U). Using Eqs. (2) and (4) it can readily be seen that:

$$|w|/|u'| = \lambda_z/\lambda_x .$$

From Figs. 1(b) and (d), a rough visual estimate indicates $|w| \simeq 5$ m/s and $|u'| \simeq 12$ m/s suggesting that the horizontal wavelength should be between two and three times larger than the vertical wavelength which compares plausibly with the above aspect ratios when U=18, 20 and 25 m/s. Accepting 16 Km. to be the horizontal wavelength, one may now compute the vertical wavelength that the disturbance would have in the troposphere using Eq. 3. A 'back of the envelope' estimate of N and U averaged between 6.5 and 9 Km. gives $N \simeq 8.10^{-3}$ s^{-1} and $U \simeq 36$ ms^{-1} so that

$$N/U \simeq 2.2.10^{-4} < k \ (\simeq 3.9.10^{-4})$$

which implies that $m^2 < 0$ i.e. the wave would be trapped in the troposphere. If, however, the height variation of the wind profile is taken into account, m is given by:

$$m^2 = (N/U)^2 - U_{zz}/U - k^2$$

and a rough estimate shows m to be close to zero. As is evident in the numerical calculations of stratified flow over two-dimensional orography made by Sawyer (1960), wave energy is capable of penetrating 3 or 4 Km. deep layers in which m^2 is close to zero. Wave energy is radiated upwards as a stationary wavetrain whose slope (dz/dx) is m/k to a high degree of

approximation(Gill,1982).Therefore,the fact that m is effectively zero in the middle and upper troposphere may explain why the gravity wave was found around 40 - 50 Km. downstream of significant orography(height greater than 400 m ,Fig.2).In Sawyer's calculation for a 'typical' airstream (his Fig.3),the lower stratospheric disturbance occurs 10 - 20 Kms. downstream.It is therefore possible that the tropospheric response in our observational study was resonant and ducted downstream whilst leaking energy to the stratosphere(Berkshire and Warren,1970) .

(c) Stationary,inertia-gravity wave

So far it has been tacitly assumed that air parcels pass through a horizontal wavelength of the disturbance on a time scale very much shorter than the pendulum day ($2\pi/f$ where f is the Coriolis parameter).If this is not the case ,the dispersion relation for m (Gill(1982) is:

$$m=Nk/((Uk)^2-f^2)^{1/2} \qquad \text{-----(16)} .$$

Assume initially that $m_*=m$,then from Fig.1(a), $m=2\pi/2.7$Km.and with $f=1.21.10^{-4}\ s^{-1}$,Eq.16 gives:

$$k=5.2.10^{-6}\ m^{-1}$$

which implies a horizontal wavelength of about 1200 Km.The neglect of the term Uk/W in Eq.13 can now be confirmed *a posteriori*.It is clear however from (b) that the very small aspect ratio of this wave is

inconsistent with the observed ratio of |u'| and |w| and so this type of very long wave could not possibly explain the observed wave.

(d) Transient, hydrostatic gravity wave

The dispersion relation for travelling internal gravity waves is obtained by replacing U in Eq.3 by U-c where c is the horizontal phase speed. For hydrostatic waves the vertical wavenumber m then satifies:

$$m=N/(U-c) \qquad \text{--------(17)} \quad .$$

The analysis in (b) is valid for travelling waves if U is interpreted as (U-c). Since a fair range of U values appear to give an aspect ratio of ≈3, c could easily lie within the range -5 to +5 m/s without greatly altering the analysis interpretation.

The wave-breaking criterion Eq.5 can be used estimate a critical temperature amplitude δT_c at which a gravity wave saturates. If we assume that the undisturbed lower stratosphere is isothermal then an adiabatic vertical displacement 'a' causes a temperature perturbation of Γa where Γ is the dry adiabatic lapse rate. The critical temperature perturbation amplitude for a travelling gravity wave is then given by:

$$\delta T_c=\Gamma(U-c)/N \qquad \text{------(18).}$$

Taking $N=2.12.10^{-2}$ m^{-1}, c=0 and $\Gamma=9.8^{o}K.Km^{-1}$. then the values U=18, 20, 25 and 30 m/s imply $\delta T_c=8.3, 9.2, 11.5$ and $13.9^{o}K$ respectively : somewhat larger than the temperature fluctuation seen in Fig.1(a).

4. Discussion

The evidence presented in Section 3 strongly suggests that the disturbance appearing in the 2318 GMT December 13 Shanwell ascent was a quasi-stationary internal gravity with horizontal and vertical wavelengths of ≃16 and 6 Km. respectively. The wave was of considerable amplitude causing a lower stratospheric temperature perturbation of ≃8°K - only slightly smaller than the critical amplitude for wave saturation when U=20 m/s.

The negative correlation of u' and w' indicate that the gravity wave was accompanied by a downward momentum flux whose magnitude may be crudely estimated as follows. The fluctuation in the rate of ascent of the balloon indicates a vertical velocity amplitude of about 4 m/s. With $|u'| \simeq 12$ m/s and an air density(ρ) at 16 Km. of 0.16 Kg m^{-3}, a mean vertical momentum flux $\rho\overline{u'w'} \simeq$ 3-4 Nm^{-2} is obtained where a factor of ½ has been included to account for averaging over one wavelength. This is, indeed, a very substantial flux of momentum (cf. 0.1 Nm^{-2} for a typical surface frictional stress) and implies a powerful influence on the lower stratospheric flow albeit over a limited area. Aircraft studies of gravity wave activity over Scotland described by Brown(1983) have revealed waves of horizontal wavelength≃20Km. and downward momentum flux≃0.4Nm^{-2} - substantially smaller than the value found here. Brown found that u'w' could be of the order of 10 to 100 times larger than the mean along the aircraft sampling trajectory(≃200 Km. in length) implying that the assumed correlation factor of ½ could be too generous. Even so it is difficult to imagine this factor being in error by one order of magnitude. Our mean momentum flux is essentially an average over one wavelength and therefore about 10 times shorter than the averaging

length in Brown's study. Combined with the fact that this was an exceptional event in the experience of the staff at Shanwell, the size of the momentum flux is probably genuine.

It has for some time been speculated that the influence of orographically forced gravity waves should be incorporated into numerical weather prediction models. Recent work by Boer et al(1984), Palmer et al(1986) and McFarlane(1986) has reemphasised this need and shows how a systematic tendency for excessive westerly flow in numerical models with high resolution can be greatly alleviated by the parametrization of gravity wave drag. Our study certainly supports this viewpoint though has obviously focused on a very extreme event.

Reid(1972) estimated that gravity waves of displacement amplitude greater than 100 m. are observed at Shanwell(at a height of 14 Km.) on ≈2% of occasions. Unfortunately his deduced amplitudes correspond to the factor aUk/χ in Eq. 11 which is smaller than the true amplitude 'a'. For the wave considered here this apparent amplitude is about half of the true amplitude and so constitutes a serious quantitative error. If a factor of two was typical of the underestimation of wave amplitude in his study then the above 2% would become 10%. Since upward propagating gravity waves typically radiate a few tens of kilometres downstream of the orography forcing them, many radiosonde ascents at Shanwell would miss the major wave activity in the lower stratosphere: balloons must frequently blow away from the Scottish Highlands over the North Sea. It would be interesting to repeat Reid's study using the true displacement amplitude and eliminating cases where the balloon is over the sea while in the lower stratosphere.

5. Conclusions

The study presented here demonstrates the potential that operational radiosonde soundings present for analysing the structure of stationary, orographic gravity waves. Using a long period of routine radiosonde observations , it may be possible to build up a picture of the frequency and geographical distribution of gravity wave breaking in the lower stratosphere from archived high resolution data. This might be sufficient to permit the verification of gravity wave drag parametrization schemes now being used in operational numerical weather prediction models. By looking for a combination of fluctuations in the temperature and balloon ascent rate it may be possible to identify other sources of gravity wave activity in the lower stratosphere such as cumulonimbus convection. Soundings obtained from ocean weather ships are unlikely to contain gravity wave contributions (in the lower stratosphere) from orography and so such events could be correlated with , for instance, active convection or regions of rapid geostrophic adjustment. The appearance of nearly isentropic layers in the lower stratosphere does not necessarily imply that the balloon has passed through a gravity wave since , as shown in section 2(b) , this may simply be the signature of an upstream wavebreaking event which has locally mixed the potential temperature of a layer within the gravity wave. Fluctuations in the ascent rate and wind speed are an essential part of the identification of gravity wave activity.

Legends

Fig.1 Radiosonde ascent profiles at Shanwell, 12 Dec. 1986 2318 GMT:

(a) Temperature (°C and potential temperature (°K)

(b) Wind speed (ms^{-1})

(c) Wind direction (degrees)

(d) Rate of ascent, computed from the geopotential(solid); computed computed from radar data(dashed and offset by $-4ms^{-1}$).

Fig.2 Balloon trajectory for Shanwell ascent at 2318 GMT, 12 Dec. 1986.

Fig.3 Sea-level pressure field at 00Z, Dec. 13, 1986. Contour interval: 2 mb.

Fig.4 Temperature(°C) for a sequence of ascents at Shanwell launched at:

(a) 1117 GMT 12 Dec. 1986

(b) 2318 ,, ,, ,,

(c) 1118 GMT 13 Dec. 1986.

Fig.5 Sequence of ascents at Shanwell showing wind speed (ms^{-1}) and launched at:

(a) 1117 GMT 12 Dec. 1986

(b) 2318 GMT ,, ,,

(c) 0515 GMT 13 Dec. 1986

(d) 1118 GMT ,, ,, ,,.

Fig.6 Radiosonde ascent profiles at Long Kesh, 12 Dec. 1986, 2326 GMT:

(a) Temperature (°C)

(b) Wind speed (ms^{-1})

(c) Wind direction (degrees).

Fig.7 Radiosonde ascent profiles at Aughton, 13 Dec. 1986, 0008 GMT:

(a) Temperature (°C)

(b) Wind speed (ms^{-1})

(c) Wind direction (degrees).

Fig.8 Steady state streamlines computed for uniform flow over a bell-shaped mountain(taken from Lilly and Klemp,1979-their Fig.5).The cross marks the position where the flow is just short of convective instability.The flow goes from left to right.

Fig.9 Potential temperature variation in a sinusoidal gravity wave at saturation amplitude measured along the vertical (solid) and following an idealised radiosonde balloon (dashed).Flow parameters and ascent rate are specified in the text.

References

Boer, G.J., McFarlane, M.A., Laprise, R., Henderson, J.D. and Blanchet, J.P. (1984) 'The Canadian Climate Centre spectral atmospheric general circulation

Brown, P.R.A. (1983) 'Aircraft measurements of mountain waves and their associated flux over the British Isles'. Quart. Roy. Met. Soc., 109, 849-866.

Corby, G.A (1957) 'A preliminary study of atmospheric waves using radiosonde data' Quart. J. Roy. Met. Soc., 83, 49-60.

Danielsen, E.F. (1959) 'The laminar structure of the atmosphere and its relation to the concept of a tropopause'. Arch. Met. Bioklim., 11, 293-332.

Edge, P., Kitchen, M., Harding, J.H. and Stancombe, J. (1986) 'The reproducibility of RS3 radiosonde and Cossor WF MkIV radar measurements' OSM 35, Meteorological Office, Bracknell.

Gill, A.E. (1982) 'Atmosphere-Ocean Dynamics' Academic Press, International Geophysics Series, Vol. 30.

Lalas, D.P. and Einaudi, F. (1980) 'Tropospheric gravity waves: their detection and influence on rawinsonde balloon data'. Quart. J. Roy. Met. Soc., 106 855-864.

Lilly, D.K. and Kennedy, P.J. (1973) 'Observations of a stationary mountain wave and its associated momentum flux and energy dissipation'. J. Atmos. Sci., 30, 1135-1152.

Lilly, D.K. and Klemp, J.B. (1979) 'The effects of terrain shape on nonlinear, hydrostatic mountain waves'. J. Fluid Mechs., 95, 241.

McFarlane, N.A. (1986) 'The effect of orographically excited gravity wave drag on the general circulation of the lower stratosphere and troposphere ' J. Atmos. Sci. (to appear)

Nash, J. and Schmidlin F.J. (1987) 'Final report on the WMO International Radiosonde Comparisons', to be published by WMO as Instruments and Methods of Observation, Report No 30.

Nicholls, J.M. (1973) 'The airflow over mountains'. WMO, Technical Note No. 127, Geneva.

Palmer, T.N. Shutts, G.J. and Swinbank, R. (1986) 'Alleviation of a systematic westerly bias in general circulation and numerical weather prediction models through an orographic gravity wave drag parametrization'. Quart. J. Roy. Met. Soc., 112, 1001-1039.

Reid, S.J. (1972) 'An observational study of lee waves using radiosonde data'. Tellus, 24, 593-596.

Sawyer, J.S. (1960) 'Numerical calculation of the displacements of a stratified airstream crossing a ridge of small height'. Quart.J.Roy.Met.Soc., 86, 326-345.

Sawyer, J.S. (1961) 'Quasi-periodic wind variations with height in the lower stratosphere'. Quart.J.Roy.Met.Soc., 87, 24-33.

Scorer, R.S. (1953) 'Theory of airflow over mountains.2- the flow over a ridge'. Quart. J. Roy. Met. Soc., 75 , 70-83.

Scorer, R.S. (1979) 'One further remark on blocking'. Weather , 34 , 361-363.

Fig. 1

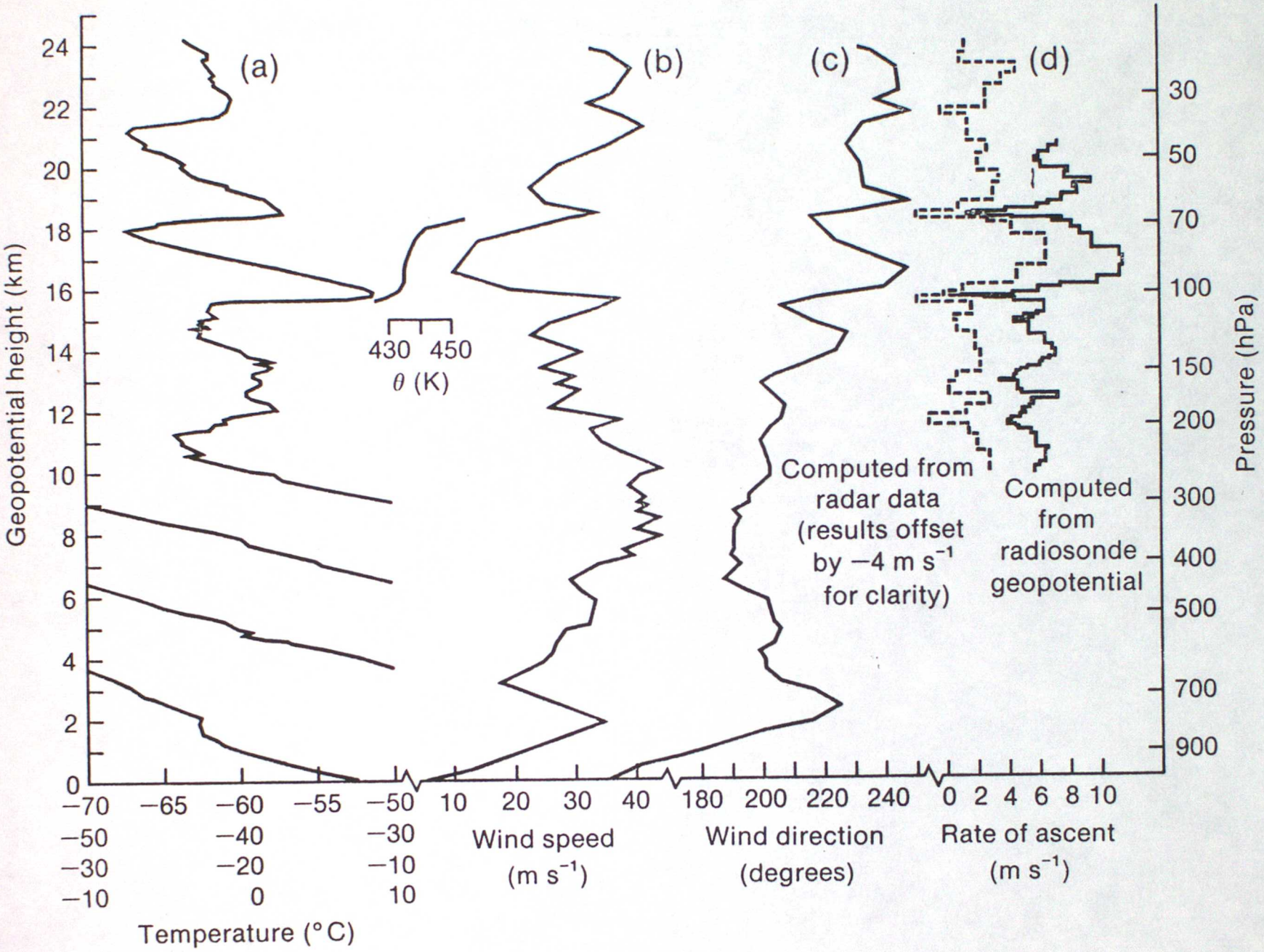
(a)
(b)
(c)
(d)
Geopotential height (km)
Pressure (hPa)
30
50
70
100
150
200
300
400
500
700
900
430 450
θ (K)
Computed from radar data (results offset by −4 m s⁻¹ for clarity)
Computed from radiosonde geopotential
−70 −65 −60 −55 −50
−50 −40 −30
−30 −20 −10
−10 0 10
Temperature (°C)
10 20 30 40
Wind speed (m s⁻¹)
180 200 220 240
Wind direction (degrees)
0 2 4 6 8 10
Rate of ascent (m s⁻¹)

Fig. 2

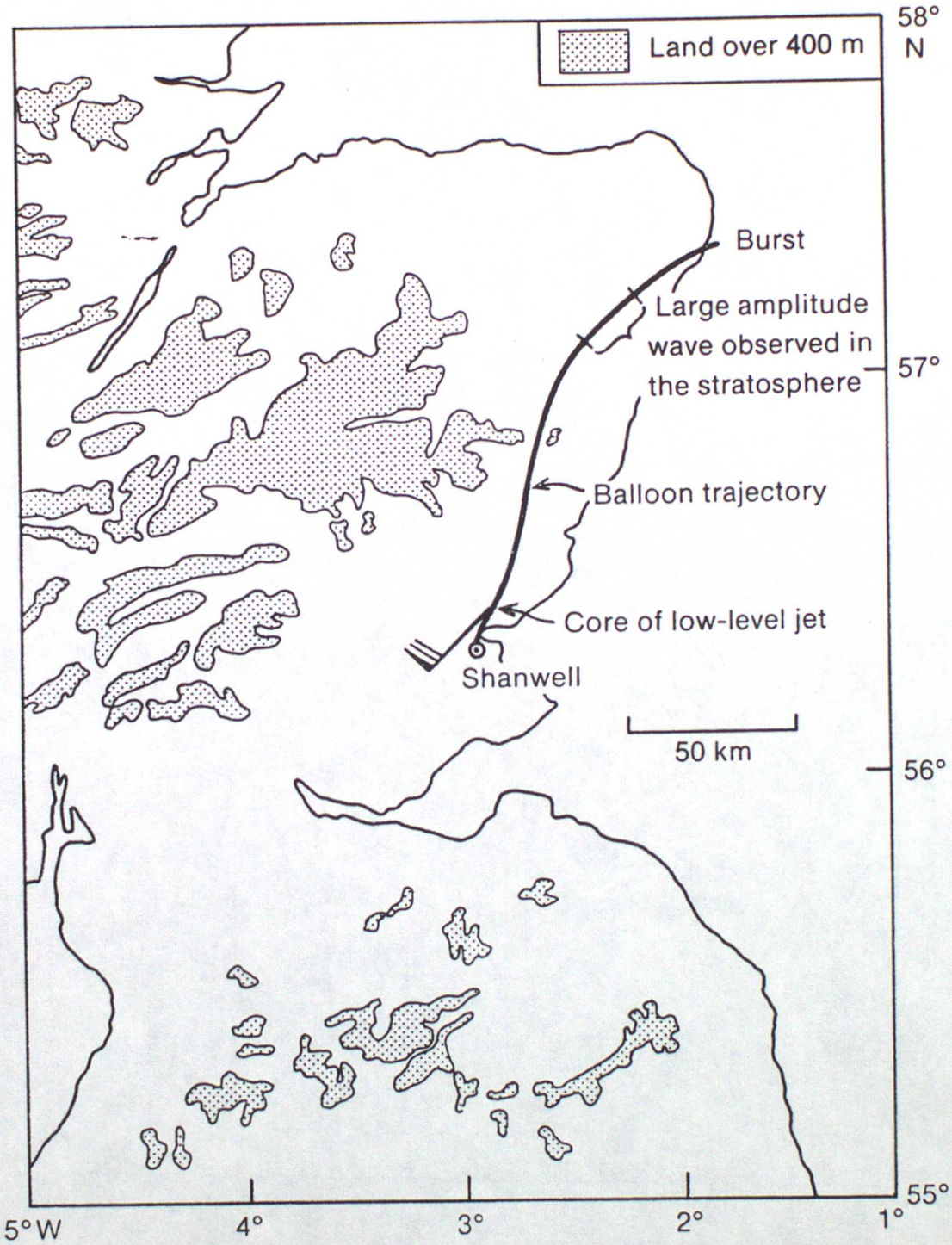
Land over 400 m
58° N
Burst
Large amplitude wave observed in the stratosphere
57°
Balloon trajectory
Core of low-level jet
Shanwell
50 km
56°
55°
5° W
4°
3°
2°
1°

Fig. 3

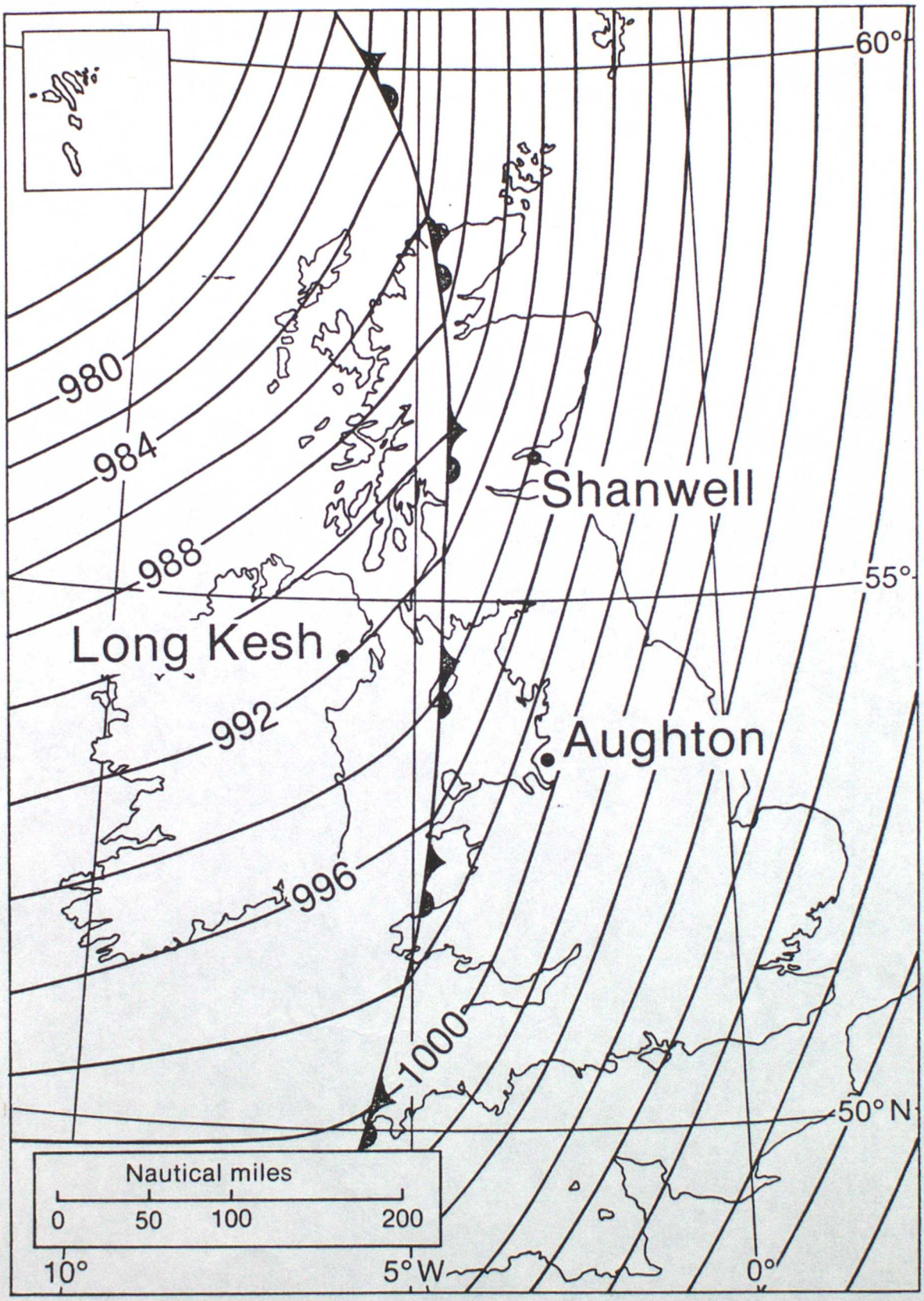
60°
980
984
988
992
996
1000
Shanwell
55°
Long Kesh
Aughton
50° N
Nautical miles
0
50
100
200
10°
5° W
0°

Fig. 4

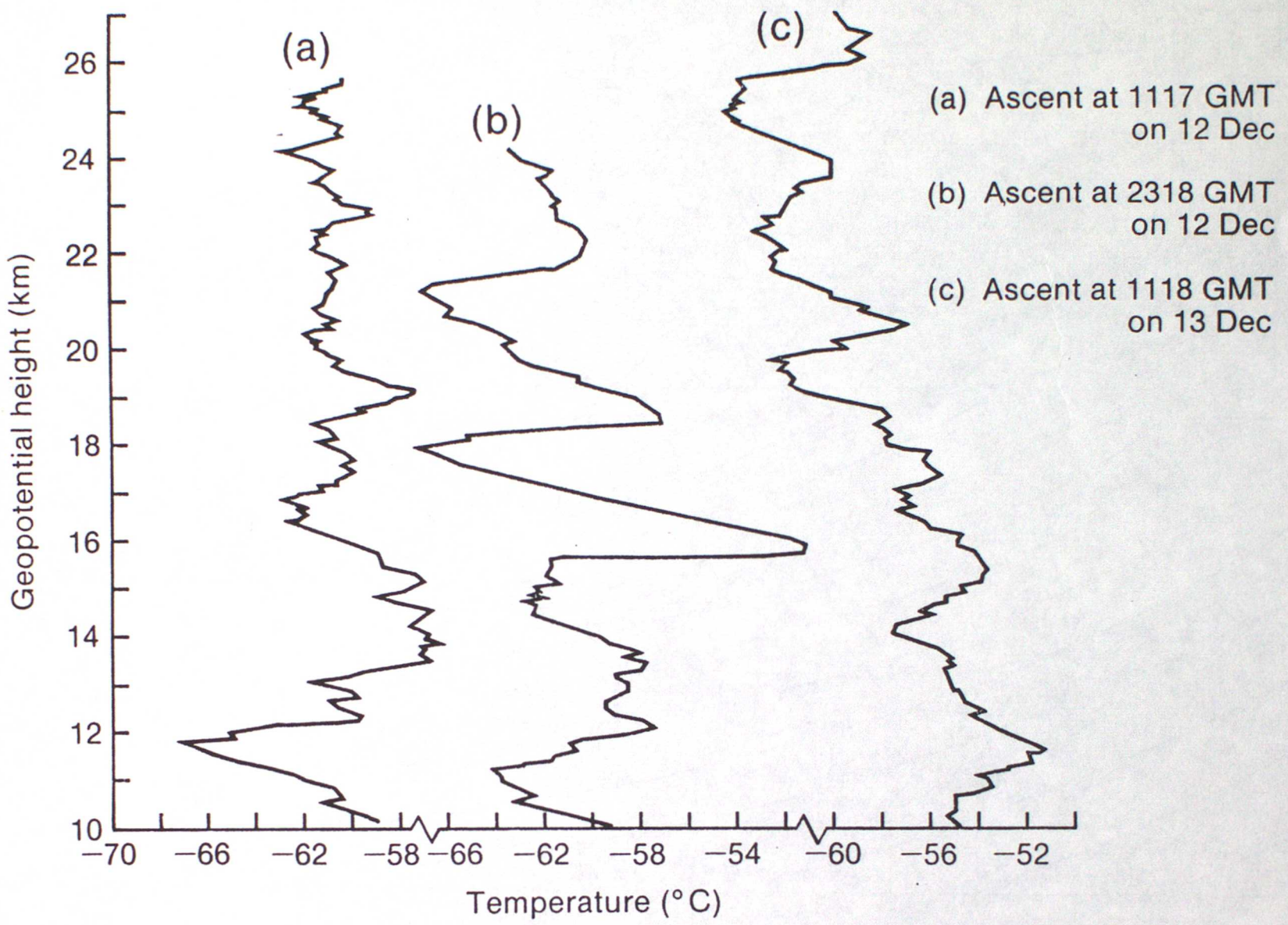
(a)
(b)
(c)
Geopotential height (km)
26
24
22
20
18
16
14
12
10
−70
−66
−62
−58
−66
−62
−58
−54
−60
−56
−52
Temperature (°C)
(a) Ascent at 1117 GMT on 12 Dec
(b) Ascent at 2318 GMT on 12 Dec
(c) Ascent at 1118 GMT on 13 Dec

Fig. 5

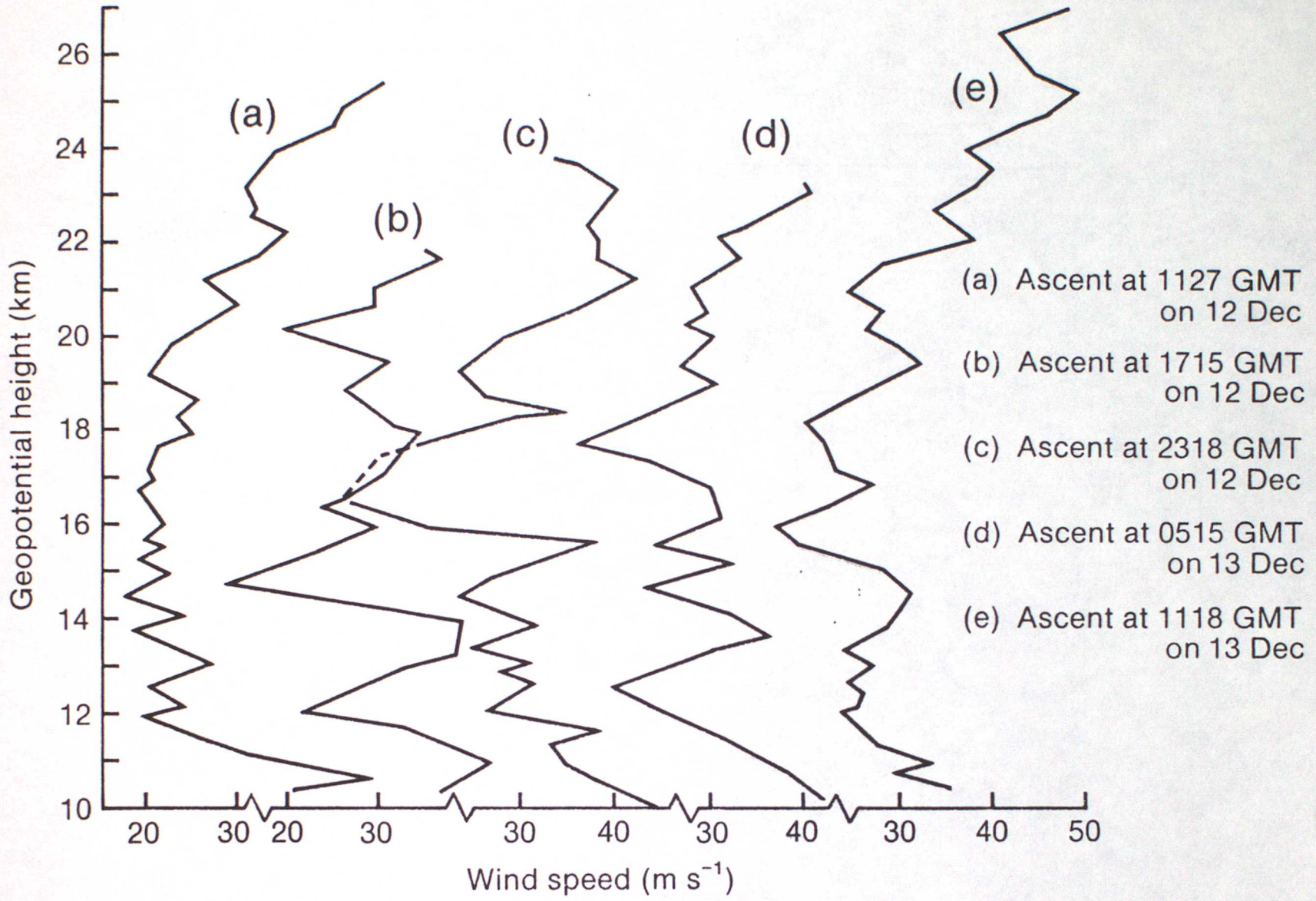
Geopotential height (km)
26
24
22
20
18
16
14
12
10
(a)
(b)
(c)
(d)
(e)
20
30
20
30
30
40
30
40
30
40
50
Wind speed (m s^{-1})
(a) Ascent at 1127 GMT on 12 Dec
(b) Ascent at 1715 GMT on 12 Dec
(c) Ascent at 2318 GMT on 12 Dec
(d) Ascent at 0515 GMT on 13 Dec
(e) Ascent at 1118 GMT on 13 Dec

Fig. 6

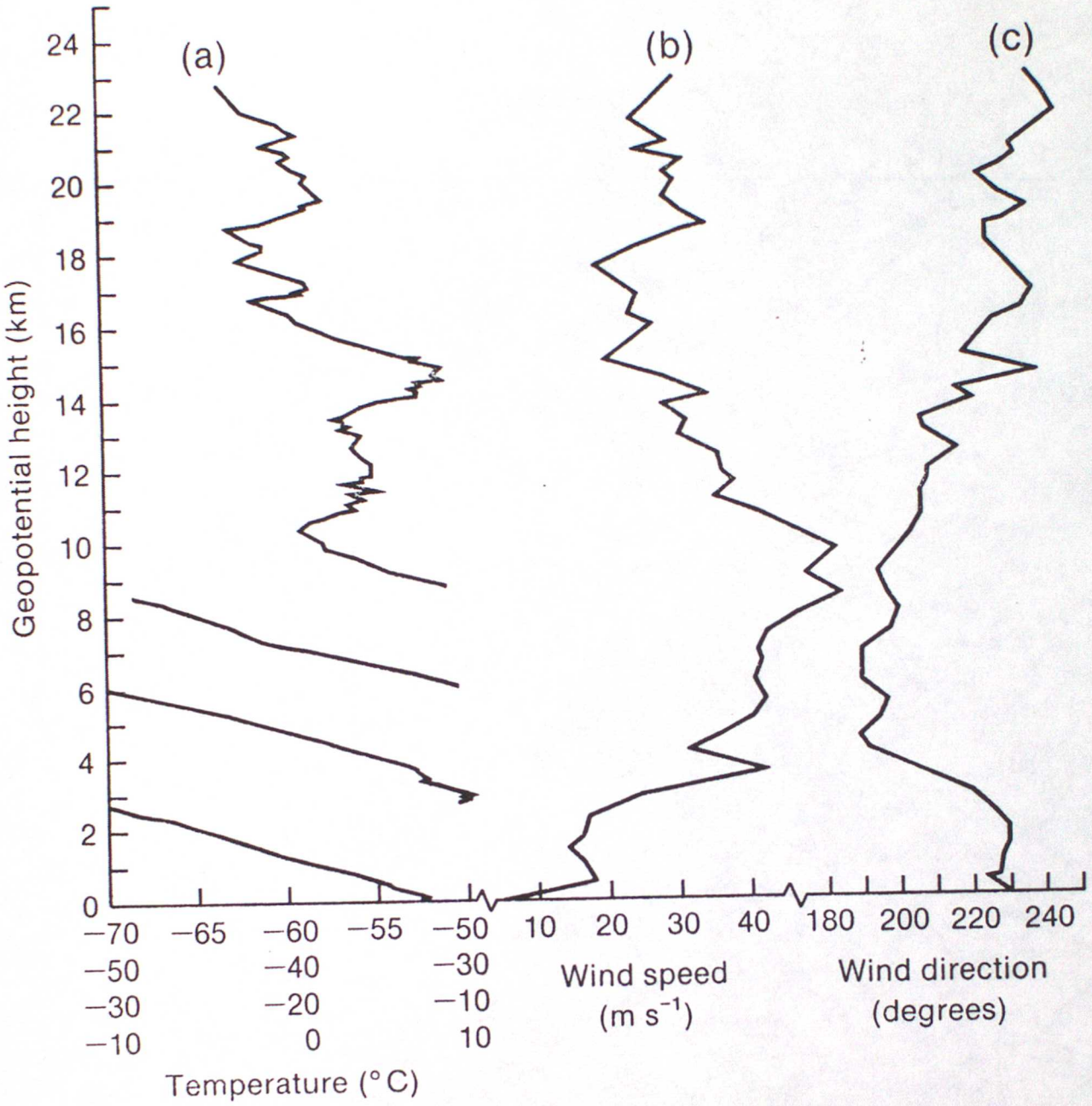
(a)
(b)
(c)
Geopotential height (km)
24
22
20
18
16
14
12
10
8
6
4
2
0
−70 −65 −60 −55 −50
−50 −40 −30
−30 −20 −10
−10 0 10
Temperature (°C)
10 20 30 40
Wind speed
(m s⁻¹)
180 200 220 240
Wind direction
(degrees)

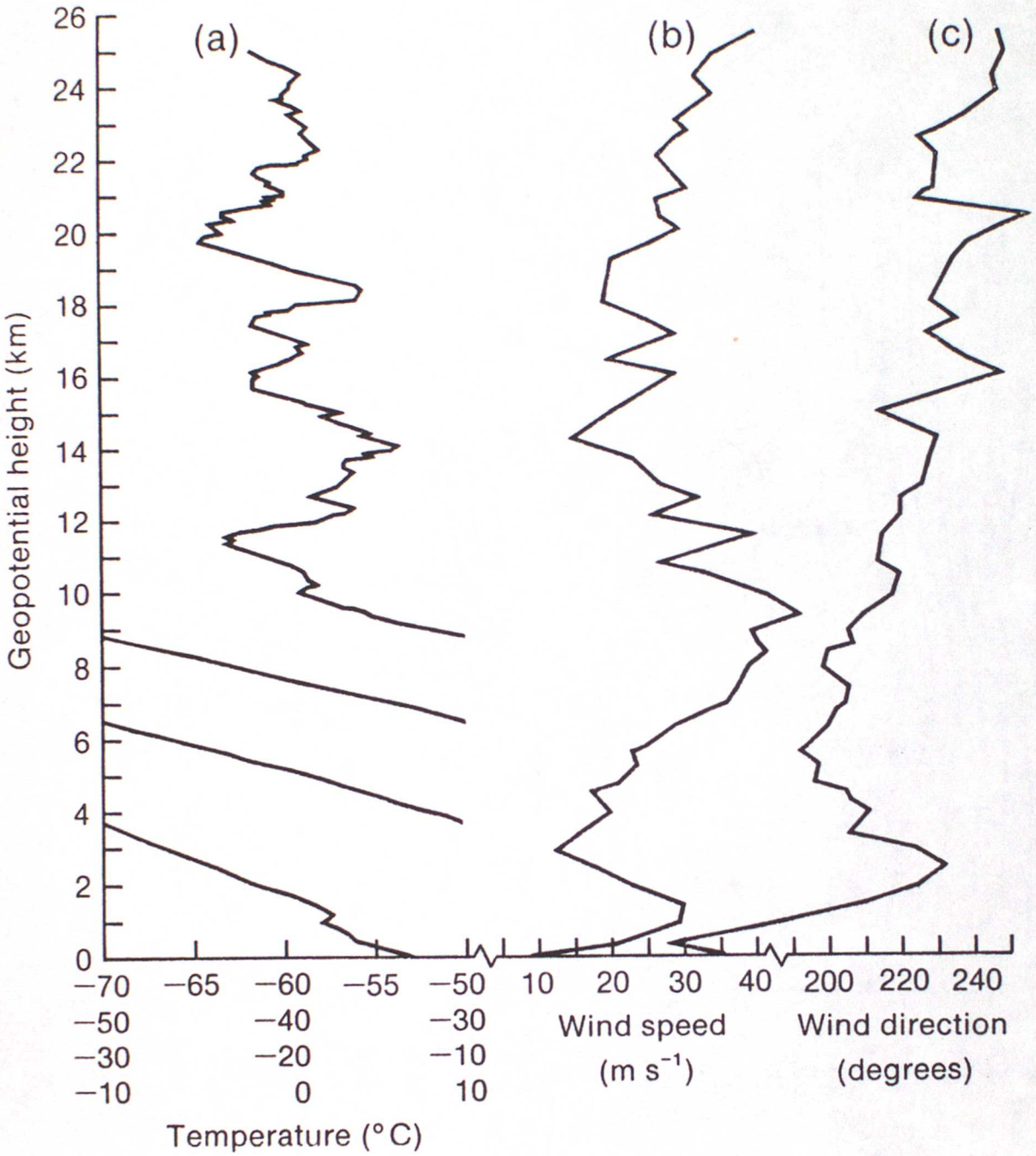
(a)
(b)
(c)
Geopotential height (km)
26
24
22
20
18
16
14
12
10
8
6
4
2
0
−70 −65 −60 −55 −50
−50 −40 −30
−30 −20 −10
−10 0 10
Temperature (°C)
10 20 30 40
Wind speed
(m s⁻¹)
200 220 240
Wind direction
(degrees)

Fig. 8

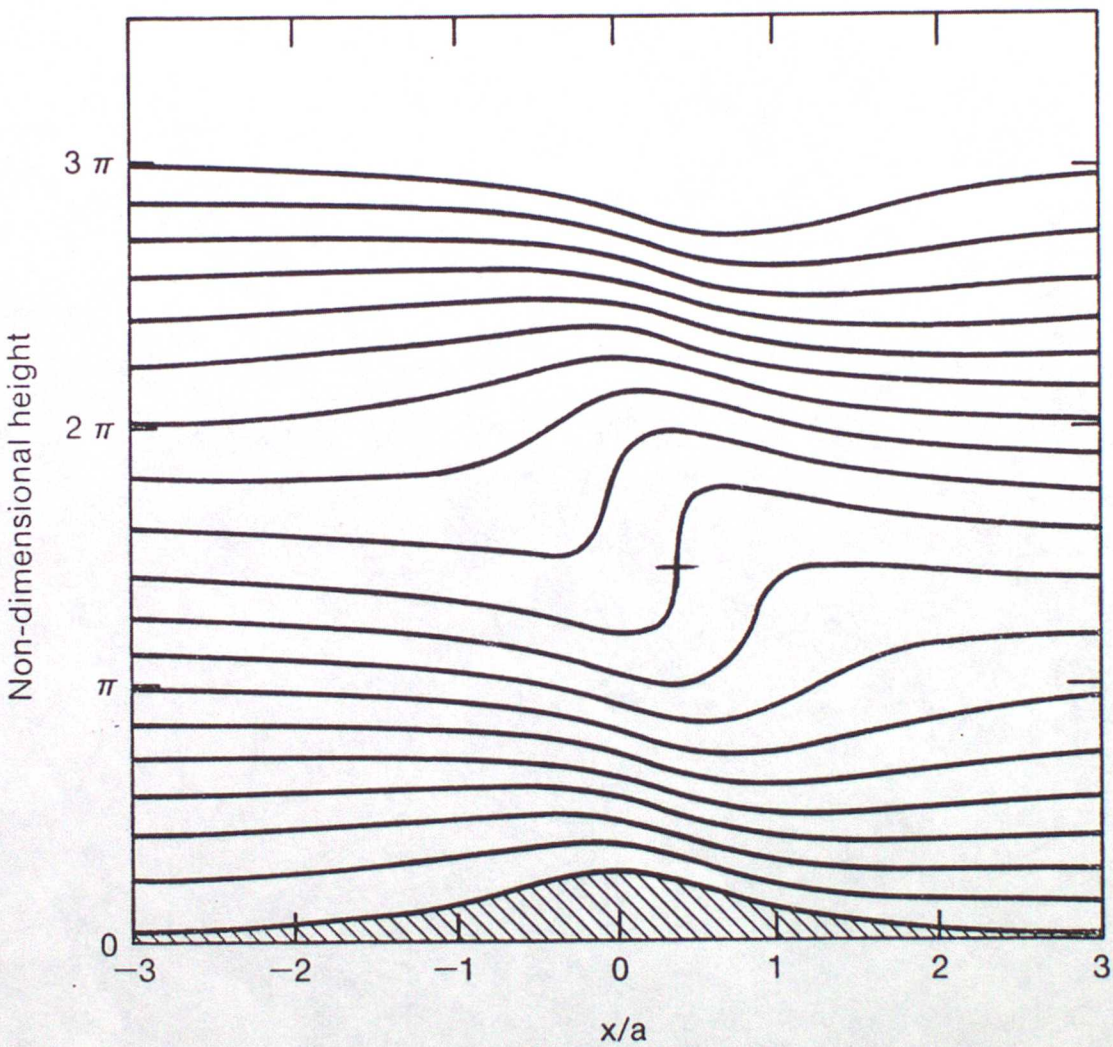

Fig. 9

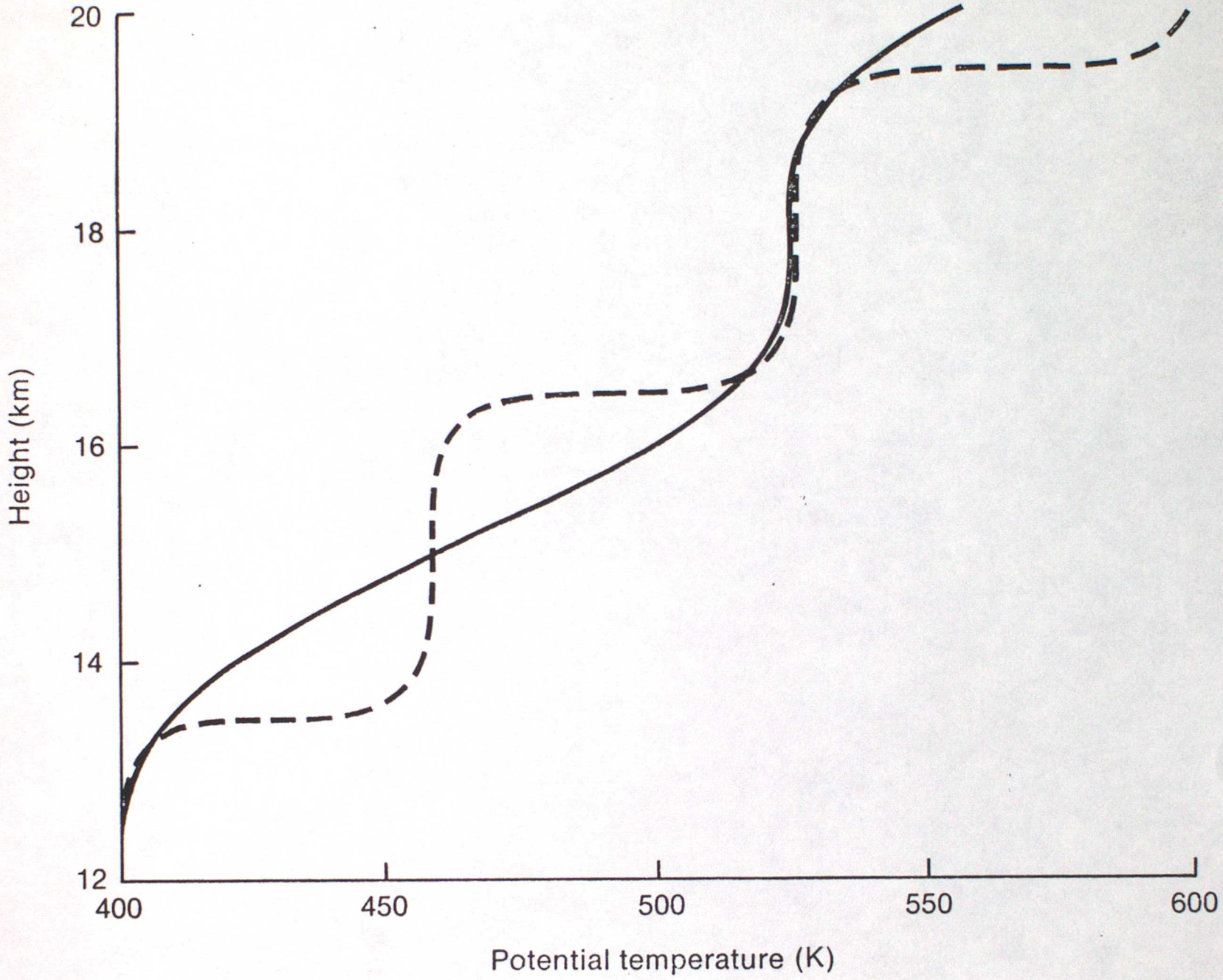
20
18
16
14
12
Height (km)
400
450
500
550
600
Potential temperature (K)